

# Pressure Induced Effects on the Fermi Surface of Superconducting 2H-NbSe<sub>2</sub>

H. Suderow,<sup>1</sup> V. G. Tissen,<sup>2</sup> J. P. Brison,<sup>3</sup> J. L. Martínez,<sup>2</sup> and S. Vieira<sup>1</sup>

<sup>1</sup>*Laboratorio de Bajas Temperaturas, Departamento de Física de la Materia Condensada, Instituto de Ciencia de Materiales Nicolás Cabrera, Universidad Autónoma de Madrid, 28049 Madrid, Spain*

<sup>2</sup>*Consejo Superior de Investigaciones Científicas, Instituto de Ciencia de Materiales de Madrid, 28049 Madrid, Spain*

<sup>3</sup>*Centre des Recherches sur les Très Basses Températures CNRS, BP 166, 38042 Grenoble Cedex 9, France*

(Received 21 April 2005; published 9 September 2005)

The pressure dependence of the critical temperature  $T_c$  and upper critical field  $H_{c2}(T)$  has been measured up to 19 GPa in the layered superconducting material 2H-NbSe<sub>2</sub>.  $T_c(P)$  has a maximum at 10.5 GPa, well above the pressure for the suppression of the charge density wave (CDW) order. Using an effective two-band model to fit  $H_{c2}(T)$ , we obtain the pressure dependence of the anisotropy in the electron-phonon coupling and Fermi velocities, which reveals the peculiar interplay between CDW order, Fermi surface complexity, and superconductivity in this system.

DOI: 10.1103/PhysRevLett.95.117006

PACS numbers: 74.70.Ad, 74.25.Dw, 74.25.Op, 74.62.Fj

2H-NbSe<sub>2</sub> is a member of the family of the 2H transition metal dichalcogenides, which is currently revisited from an experimental and theoretical point of view. The invention of the scanning tunneling microscope and its application to the study of the local density of states of superconductors has revealed important fundamental properties of the superconducting state of 2H-NbSe<sub>2</sub>. The internal structure of the vortex cores was unveiled in Refs. [1,2], an unusual strong gap anisotropy was found in Ref. [2], and it was also found that the superconducting and charge density wave (CDW) orders, with, respectively,  $T_c = 7.1$  K and  $T_{\text{CDW}} = 32$  K [3,4], coexist at the local level. However, the delicate balance that threads strong anisotropy, superconductivity, and CDW ordering, probably one of the most intriguing questions, is still elusive.

The arena of this debate is the Fermi surface (FS). A notable experimental effort has been done recently to measure the FS by angular resolved high resolution photoemission spectroscopy (ARPES) [5–9]. These experiments, backed by band structure calculations [10,11], have provided new insight to analyze the relevance of the existing theoretical proposals for the mechanisms in the origin of the CDW state (see, e.g., [12,13]). They have also found that 2H-NbSe<sub>2</sub> is a multiband superconductor with some intriguing similarities to the magnesium diboride (MgB<sub>2</sub>) the archetype of this kind of superconductivity [14]. Actually, the FS of 2H-NbSe<sub>2</sub> consists of three main bands crossing the Fermi level [5–11]. Two of them derive from the Nb 4d orbitals and result in two cylindrical sheets with a small dispersion along the *c* axis (2D). A relatively large and homogeneous superconducting gap is found in this part of the FS ( $\Delta = 0.9$ –1 meV), with electron-phonon coupling parameters that differ in each sheet between  $\lambda \approx 1.7$  in one cylinder and  $\lambda \approx 0.8$  in the other [8,9]. The third band derives from Se 4p orbitals and gives a small pancake like (3D) FS centered around the  $\Gamma$  point with much weaker electron-phonon coupling ( $\lambda \approx 0.3$ ) and a small superconducting gap, which is below the experimental resolution of Ref. [8]. Further evidences supporting multi-

band superconductivity come from thermal conductivity experiments under magnetic fields as well as superconducting tunneling spectroscopy [15,16].

Pressure is a thermodynamic parameter which is believed to have strong influence on the electronic properties of 2H-NbSe<sub>2</sub>, due to the big interlayer distance and the small interaction between them. We can obtain direct access under pressure to important FS parameters through the measurement of the upper critical field  $H_{c2}(T)$ . Indeed, since the seminal work of Hohenberg and Werthammer [17], it is known that the orbital limitation of  $H_{c2}(T)$  is mainly controlled by the Fermi velocity  $v_F$ . As a consequence,  $H_{c2}(T)$  can appreciably deviate from the usual (almost parabolic) behavior in clean superconductors when the various sheets of the FS have different electron-phonon coupling parameters and Fermi velocities. In such a case, an eventually complex FS can often be modeled by just two bands, allowing to extract the main anisotropies in  $\lambda$  and  $v_F$  from  $H_{c2}(T)$  [18,19]. In a previous article we have measured the pressure evolution of the critical temperature  $T_c$  and upper critical field  $H_{c2}(T)$  of two topical superconductors, MgB<sub>2</sub>, and the nickel borocarbide YNi<sub>2</sub>B<sub>2</sub>C, and obtained the pressure induced changes on  $\lambda$  and  $v_F$  using such an effective two-band model [20]. In this Letter we use the same approach in 2H-NbSe<sub>2</sub>, and find a very strong effect of pressure on the FS.

We measured small single crystalline samples of 2H-NbSe<sub>2</sub>, which were previously used in local tunneling spectroscopy studies of the superconducting density of states and the CDW [16]. Samples were cut to a size of  $0.12 \times 0.12 \times 0.03$  mm<sup>3</sup> and loaded into the pressure cell. The pressure was determined using the ruby fluorescence method and the transmitting medium was a methanol-ethanol mixture, which is thought to give quasihydrostatic pressure conditions. However, we did verify that, in MgB<sub>2</sub>,  $T_c(P)$  is the same, up to the highest pressures (20 GPa), as in measurements made by other groups under hydrostatic conditions ( $dT_c/dP = -1.1$  K/GPa), i.e., using helium as a pressure transmitting medium, so that deviations from

hydrostatic conditions should not influence the results found with this method.  $T_c(P)$  and  $H_{c2}(T)$  were obtained by measuring, at each pressure, the magnetic susceptibility as a function of temperature and at different magnetic fields, always applied perpendicular to the layers, as shown by several representative scans in Fig. 1. The susceptometer was described in Ref. [20]. Note that ambient pressure  $H_{c2}(T)$  obtained with this method is in good agreement with previous work in NbSe<sub>2</sub> [21].

Let us discuss the pressure dependence of the critical temperature, shown as points in Fig. 2. Previous experiments have measured  $T_c(P)$  up to 5 GPa [22–24]. It has been shown that the application of hydrostatic pressure results in a continuous increase of  $T_c(P)$  followed by a decrease of  $T_{CDW}$ , which is suppressed at about 5 GPa. Here we find the same behavior for  $T_c(P)$  as already reported below 5 GPa, an increase of  $T_c$  with a slope of  $dT_c/dP = 0.25$  K/GPa. Between 5 GPa and 10.5 GPa  $T_c$  increases by a small amount ( $dT_c/dP = 0.05$  K/GPa), followed by a decrease above 10.5 GPa ( $dT_c/dP = -0.1$  K/GPa).

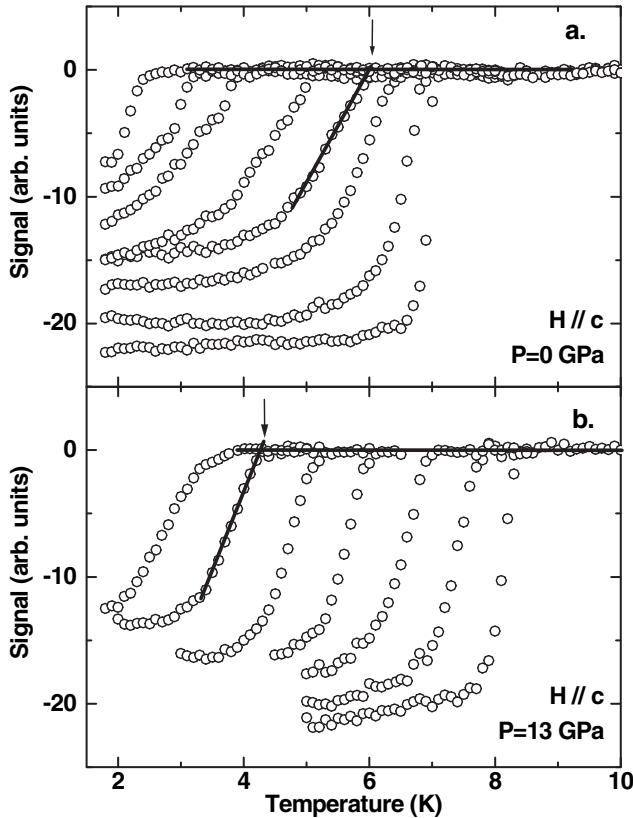


FIG. 1. A characteristic example of the measured temperature dependence of the susceptibility at several fixed magnetic fields for two pressures (a) at ambient pressure and, from right to left, 0, 0.05, 0.3, 0.7, 1.5, 2.5, 3.3 T; and (b) at 13 GPa and 0, 0.05, 0.2, 0.4, 0.6, 0.8, 1.0 T). Arrows and lines demonstrate the way we extract the corresponding point in the  $H_{c2}(T)$  phase diagram (same as in [20]).

$H_{c2}(T)$  shows a peculiar temperature dependence at all pressures (Fig. 3). Very simple estimates demonstrate that the observed behavior is highly anomalous. From BCS theory, it is easily obtained that  $H_{c2}(T = 0 \text{ K}) \propto T_c^2$ . This is indeed roughly found in MgB<sub>2</sub>, where  $T_c$  drops by a factor of 2 and  $H_{c2}(T = 0 \text{ K})$  by a factor of 4 between ambient pressure and 20 GPa [20]. However in 2H-NbSe<sub>2</sub>, below 5 GPa [Fig. 3(a)],  $H_{c2}(T = 0 \text{ K})$  decreases nearly by a factor of 1.7, but  $T_c$  increases by 18%. Between 5 GPa and the maximum of  $T_c$  (10.5 GPa),  $H_{c2}(T = 0 \text{ K})$  continuously decreases [Fig. 3(b)] and  $T_c$  slightly increases by about 3%. Only above 10.5 GPa [Fig. 3(c)] the pressure induced decrease of  $T_c$  is followed by a decrease in  $H_{c2}(T = 0 \text{ K})$ .

The lines in Fig. 3 are fits of the  $H_{c2}(T)$  data using the procedure described in detail in Refs. [20,25]. Note that, as discussed in Refs. [18–20,25], from the analysis of  $H_{c2}(T)$  within an effective two-band model, one can obtain the most significant anisotropy found over the FS in  $\lambda$ . However, it is not possible to obtain independent values for the whole set of four strong coupling parameters  $\lambda_{ij}$  needed in a two-band model (interband and intraband coupling). Therefore, as in Refs. [20,25], we reduce  $\lambda_{ij}$  to only two:  $\lambda_1 = \lambda_{11}$  for the band 1 with strongest coupling and  $\lambda_2 = \lambda_{22} = \lambda_{12} = \lambda_{21}$  to characterize the more weakly coupled band 2, and its interband coupling to band 1. This approximation gives the overall pressure evolution of the anisotropy of  $\lambda$  and of  $v_F$ , although their absolute values may somewhat change in a more detailed treatment. For the ambient pressure  $H_{c2}(T)$  we fix  $\lambda_1 = 1.6$  and  $\lambda_2 = 0.16$  to obtain a corresponding overall mass renormalization  $(m_1^*/m - 1) = \lambda_{11} + \lambda_{12} = 1.76$  (strong

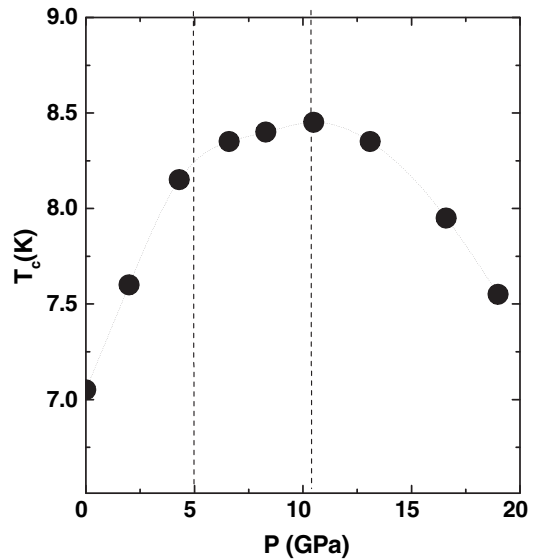


FIG. 2. The pressure dependence of the critical temperature  $T_c(P)$  measured here is shown as solid points (the line between points is a guide to the eye). Vertical dashed lines represent the pressures for the suppression of the CDW at 5 GPa, according to Refs. [22–24], and the maximum in  $T_c$  at 10.5 GPa found here.

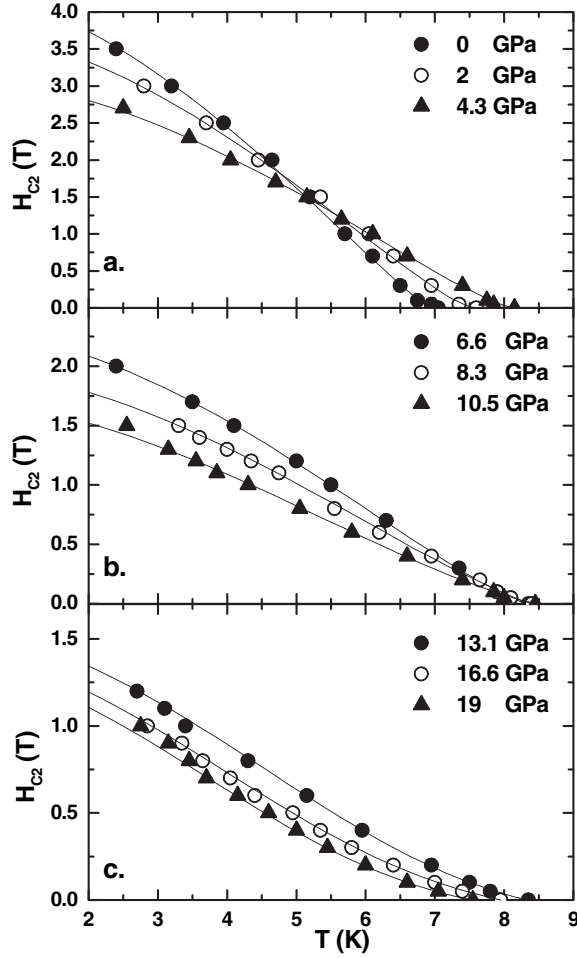


FIG. 3.  $H_{c2}(T)$  is shown up to 4.3 GPa in (a), between 6.6 and 10.5 GPa in (b) and up to 19 GPa in (c). Lines are fits to the data, using the theory described in Refs. [20,25]. Note the strong temperature dependence of  $H_{c2}(T)$  at all pressures.

coupling Nb 4d cylinders), and  $(m_2^*/m - 1) = \lambda_{22} + \lambda_{21} = 0.32$  (weak coupling Se 4p derived pocket) that compares well with the values mentioned above and obtained from de Haas–van Alphen and ARPES studies [9,11]. From the fit to  $H_{c2}(T)$ , we deduce the values of the ambient pressure unrenormalized Fermi velocities,  $v_{F,1} = 0.055 \times 10^6$  m/s and  $v_{F,2} = 1 \times 10^6$  m/s. Other parameters of the model are the Coulomb pseudopotential  $\mu^* = 0.1$ , fixed arbitrarily, and a mean phonon frequency of  $\theta = 55$  K, which is imposed to be pressure independent and is adjusted to give the right  $T_c$  at  $P = 0$ . Note, however, that changes in  $\theta$  do not have a significant influence on the form of  $H_{c2}(T)$ , which essentially depends on the anisotropy of  $\lambda_{1,2}$  and of  $v_{F,1,2}$  [18,19], whose pressure evolution is shown in Fig. 4.

We find that the initial increase of  $T_c$  with pressure (Fig. 2), is essentially controlled by that of  $\lambda_1$ , whereas  $\partial\lambda_2/\partial P$  at  $P = 0$  is close to zero (Fig. 4). Above 5 GPa,  $\lambda_1$  decreases, but  $\lambda_2$  increases up to about 11 GPa, where the maximum in  $T_c(P)$  is found. On the other hand,  $v_{F,1}$  increases under pressure up to 8.3 GPa, where a clear

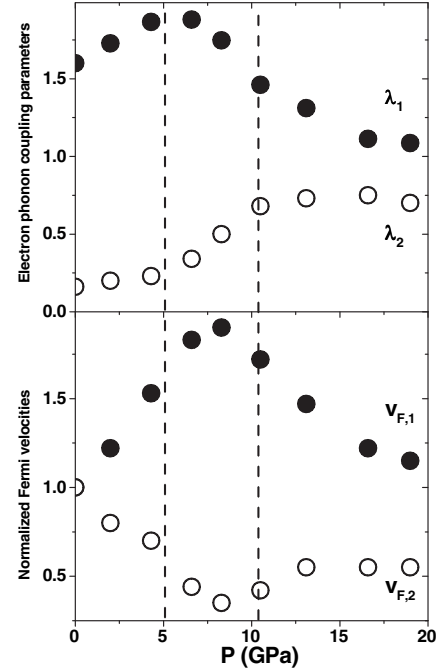


FIG. 4. Pressure dependence of the parameters of the fits shown in Fig. 3. Dashed lines indicate the suppression of the CDW at 5 GPa and the maximum in  $T_c(P)$  at 10.5 GPa. Top figure: electron-phonon coupling parameters  $\lambda_1$  (solid circles) and  $\lambda_2$  (open circles). Bottom figure: the corresponding Fermi velocities, ( $v_{F,1}$  solid circles and  $v_{F,2}$  open circles), normalized to their respective ambient pressure values.

peak is observed. The evolution of  $v_{F,2}$  is exactly opposite and becomes roughly pressure independent above 15 GPa, where the coupling strength becomes more isotropic, but the FS anisotropy remains.

Let us first discuss the evolution of the Fermi velocities, which points to a new characteristic pressure of 8.3 GPa. Anomalies on  $v_F$  might reflect changes in the Fermi surface topology. Indeed, assuming bands with a roughly quadratical dispersion, the Fermi velocities are related to their radius in  $k$  space. The eventual closing of a gap results in an increase of the area of the relevant FS, as already observed in the compound  $\text{YNi}_2\text{B}_2\text{C}$ , where the behavior of  $H_{c2}(T)$  under pressure evidences a strong increase of  $v_F$  in the strong coupling bands, related to the disappearance of a FS nesting feature under pressure [20,26,27]. On the other hand, in the case of  $\text{MgB}_2$ , the observed decrease in  $v_{F,1}$  under pressure is related to a continuous shrinking of the strong coupling sheets under pressure due to the reduction of their hole doping, achieved at zero pressure through its ionic layered character [20,28].

In  $2\text{H-NbSe}_2$ , the behavior of  $v_{F,1}$  and  $v_{F,2}$  is more intriguing. The pressure evolution of  $v_{F,1,2}$  is not changed by the disappearance of the CDW order. Instead, it peaks at 8.3 GPa, closely following the strong decrease of  $v_{F,2}$ , which stops at the same pressure. While the Nb 4d derived cylinders increase its size under pressure, the  $\Gamma$  centered pancake FS shrinks. Moreover, the whole smooth increase

of  $\lambda_2$  from 0.3 up to 0.8 at intermediate pressures reflects the progressive decrease of weight of the effect of the Se 4*p* pancake pocket on the weak coupling parameters of the effective two-band model, in favor of the Nb 4*d* cylinder which shows, at ambient pressure, intermediate coupling. The increase of  $v_{F,2}$  above 8.3 GPa then reflects, like  $\lambda_2$ , the dominant effect in  $H_{c2}(T)$  of the Nb 4*d* bands at higher pressures. So the main feature pointed out by the minimum of  $v_{F,2}$  and the increase of  $\lambda_2$  is a charge transfer from the Se 4*p* pocket, which shrinks under pressure, to the Nb 4*d*-derived cylinders, which correspondingly increase its size. This leaves only the Nb 4*d* bands control  $H_{c2}(T)$  at the highest pressures.

As regards now the evolution of the coupling parameters, the striking result from this two-band analysis is that contrary to the anomaly on the Fermi velocities (at 8.3 GPa), or the maximum of  $T_c$  (at 10.5 GPa),  $\lambda_1$  peaks at the pressure where the CDW order has been reported to vanish (5 GPa [22–24]). It is remarkable that this maximum occurs only in the strong coupling part of the FS, i.e., the Nb 4*d*-derived cylinders. The CDW gap has been reported to open on those cylinders, but not on the Se 4*p*-derived pocket [7].

Clearly, the fact that in 2H-NbSe<sub>2</sub> the suppression of the CDW order does not coincide with the maximum in  $T_c$  makes an interesting contrast with respect to a number of other systems with competing or coexisting ground states, and where  $T_c$  is maximum at a critical pressure, or doping, where another type of instability disappears. For example, in many layered high  $T_c$  superconductors, a close relationship is found between the doping dependence of  $T_c$  and of  $T^*$ , the pseudogap critical temperature (in hole doped as well as in electron doped materials, see, e.g., [29]). In the Ce heavy fermion systems under pressure [30], a maximum appears in  $T_c$  at the same pressure where the Néel temperature is suppressed, demonstrating the implications of the softening of magnetic modes in the formation of superconducting correlations. In the case of 2H-NbSe<sub>2</sub>, it would be also tempting to interpret the peak in  $\lambda_1$  in terms of some kind of mode softening near the suppression of the CDW order. However, we can equally argue that the increase in  $\lambda_1$  when  $T_{CDW}$  decreases is related to an increase of the density of states due to the pressure induced suppression of the CDW gap. In that case, clearly, the CDW ground state would be in strong competition with superconductivity. The electron-phonon coupling of the strongest coupling Nb 4*d* band would be responsible for both ground states, triggering the appearance of the CDW when approaching 5 GPa from high pressures. Our results leave both scenarios open for future debate. Nevertheless, it becomes clear that superconductivity does not have its maximum  $T_c$  when CDW order is suppressed, but when the overall coupling constant has an optimal value. This optimum results from the competition between a favorable charge transfer from the Se 4*p* band to the Nb 4*d* bands, and a decreasing electron-phonon coupling with increasing pressure.

Summarizing, our results clearly point to a maximum of the electron-phonon coupling on the FS sheet with largest  $\lambda$  at the pressure where the CDW order is suppressed. The strongly pressure dependent interplay between the electron-phonon coupling and the multiband structure of the FS, which is essential for the superconducting state, versus the FS anomalies, which are determinant for the CDW order, has been clarified through the measurement of  $T_c$  and  $H_{c2}(T)$  under pressure.

We acknowledge discussions with A. H. Castro Neto, F. Guinea, P. C. Canfield, and J. Flouquet, and support from the MCyT (Grants No. FIS-2004-02897, No. MAT-2002-1329 and No. SAB2000-039), from the Comunidad Autónoma de Madrid (07N/0053/2002) and from COST P-16.

- 
- [1] H. F. Hess *et al.*, Phys. Rev. Lett. **62**, 214 (1989).
  - [2] H. F. Hess, R. B. Robinson, and J. V. Waszczak, Phys. Rev. Lett. **64**, 2711 (1990).
  - [3] D. E. Moncton, J. D. Axe, and F. J. DiSalvo, Phys. Rev. B **16**, 801 (1977).
  - [4] J. A. Wilson, F. J. DiSalvo, and S. Mahajan, Adv. Phys. **24**, 117 (1975).
  - [5] T. Straub *et al.*, Phys. Rev. Lett. **82**, 4504 (1999).
  - [6] K. Rossmagel *et al.*, Phys. Rev. B **64**, 235119 (2001).
  - [7] W. C. Tonjes *et al.*, Phys. Rev. B **63**, 235101 (2001).
  - [8] T. Yokoya *et al.*, Science **294**, 2518 (2001).
  - [9] T. Valla *et al.*, Phys. Rev. Lett. **92**, 086401 (2004).
  - [10] J. Graebner and M. Robbins, Phys. Rev. Lett. **36**, 422 (1976).
  - [11] R. Corcoran *et al.*, J. Phys. Condens. Matter **6**, 4479 (1994).
  - [12] T. Rice and G. Scott, Phys. Rev. Lett. **35**, 120 (1975).
  - [13] A. H. Castro Neto, Phys. Rev. Lett. **86**, 4382 (2001).
  - [14] P. C. Canfield, P. Gammel, and D. Bishop, Phys. Today **51**, No. 10, 40 (1998).
  - [15] E. Boaknin *et al.*, Phys. Rev. Lett. **90**, 117003 (2003).
  - [16] J. Rodrigo and S. Vieira, Physica (Amsterdam) **404C**, 306 (2004).
  - [17] P. Hohenberg and W. Werthammer, Phys. Rev. **153**, 493 (1967).
  - [18] S. V. Shulga *et al.*, Phys. Rev. Lett. **80**, 1730 (1998).
  - [19] T. Dahm and N. Schopohl, Phys. Rev. Lett. **91**, 017001 (2003).
  - [20] H. Suderow *et al.*, Phys. Rev. B **70**, 134518 (2004).
  - [21] T. Kita and M. Arai, Phys. Rev. B **70**, 224522 (2004).
  - [22] D. Jerome *et al.*, J. Phys. (Paris), Colloq. **37**, C125 (1976).
  - [23] T. Smith, J. Low Temp. Phys. **6**, 171 (1972).
  - [24] R. E. Jones *et al.*, Phys. Rev. B **6**, 835 (1972).
  - [25] M. A. Measson *et al.*, Phys. Rev. B **70**, 64516 (2004).
  - [26] S. B. Dugdale *et al.*, Phys. Rev. Lett. **83**, 4824 (1999).
  - [27] P. Martínez-Samper *et al.*, Phys. Rev. B **67**, 014526 (2003).
  - [28] J. M. An and W. E. Pickett, Phys. Rev. Lett. **86**, 4366 (2001).
  - [29] L. Alff *et al.*, Nature (London) **422**, 698 (2003).
  - [30] N. D. Mathur *et al.*, Nature (London) **394**, 39 (1998).